Modeling The Morbidity and Mortality of Malaria Pathogenesis

R.J. Austerman

Table of Contents

Abstract……2

Introduction……2

Model……12

Analysis……14

Simulations……21

Discussion……30

Works Cited……36

Abstract

Despite the hundreds of millions of malaria cases per year and the disease's ubiquity, surprisingly little is known about the causes of malarial morbidity and mortality. Approximately 350-500 million malaria cases develop per year, and result in between 700,000 and 2.7 million deaths. However, a precursory glance at these numbers shows that mortality caused by malaria is quite rare with respect to the total number of cases. Indeed, the damage of deaths by malaria is far overshadowed by the debilitating symptoms of the disease and their effects. Patients with malaria can rarely work when infected, and the length of the infection can be anywhere from weeks to years. With such a large number of infections occurring in developing countries and the cause of this disease disabling so many workers, malaria is undeniably holding back developing countries. Thus, malaria research can benefit the world in ways other than alleviating suffering in underdeveloped regions; it can even promote economic stability and prosperity in regions across the world. Here I present a novel, in-host model of malaria pathogenesis, and look at the morbidity and mortality of an infection. I test the model's biological soundness, and run simulations with different parameter values in an attempt to see some of the differences between malarial parasites in humans.

Introduction

The numbers presented above may be more meaningful when compared with the those of a disease that currently gets much more attention and causes far more panic than malaria, HIV/AIDS. The last estimation of the total number of HIV infections was 30-36 million cases. Note that this is not the number of infections per year, but instead the sum

over a number of years. Between 2.2 and 3.2 million patients died from AIDS, making HIV infection deadlier, but far less prevalent.

The blight of malaria is a direct consequence of human actions and an unfortunately common lack of policy-making that leaves natural selection and evolution out of the picture. Poorly executed campaigns targeting the parasites that cause malaria and their mosquito vector have rendered many available immunizations and pesticides obsolete. Studies have found that the degree of drug resistance of malaria and mosquito vectors is inversely proportional to the quality of execution of these public health campaigns (Goodman *et al* 2007). Malaria is more prevalent than ever.

The disease is caused by an infection with one or a combination of the four malarial parasites that infect humans, *Plasmodium falciparum*, *ovale*, *vivax* and *malariae* (Azevedo and Portillo 2007). They are contained in the phylum *Apicomplexa*, a large group of eukaryotic protozoans. These obligate parasites are named by their characteristic apical complex, an organelle that assists in attaching and penetrating host cells. This organelle is believed to be a secondary embosymbiont, similar in origin to mitochondria.

The complex life cycles involving non-human hosts complicate the study and treatment of this parasite. *Plasmodium* are inactive outside of their hosts, and rely on female mosquitoes of the species *Anopheles* for transmission between humans. An infection with *P. falciparum* begins when a host is bitten by an infected female *Anopheles*. Sporozoites in the mosquito's salivary glands enter the host's bloodstream and quickly take refuge in the liver cells. The process of transferred sporozoites infecting host liver cells takes less than thirty minutes, and none can be found in free circulation after this time. This miniscule window of opportunity makes detection of the parasite by

the host's immune system difficult. Over the course of fourteen days, these sporozoites reproduce asexually and produce thousands of merozoites, which then leave the liver and begin infecting host red blood cells (RBCs). These merozoites can further reproduce, and have the potential to create extremely high levels of parasitemia. The cycle is completed when a female *Anopheles* feeds on this host's blood, and introduces the parasite to a new individual two days later.

P. falciparum's closest relative is *P. reichenowi*, a simian protozoan parasite. Studies using molecular clock theory suggest that the two species diverged at the same time that humans diverged from the primates (Escalante 1995). However, others have pointed out a relatively small degree of polymorphism in the species, and claim that this is evidence of *P. falciparum* being much younger (Hartl 2004). This discrepancy has been reconciled by researchers who explain that the low amount of polymorphism is a result of the parasite's recent, rapid expansion (Joy *et al* 2003).

As mentioned above, *Plasmodium falciparum, vivax, malariae,* and *ovale* all share many similarities, but also have several differences. *P. falciparum* is the most deadly species, responsible for 80% of all malarial infections and 90% of malarial deaths. It has quickly evolved in response to human treatment endeavors. Strains have become resistant to chloroquine, quinine/tetracycline combinations, and other antimalarial drugs. Studies show that different locations have strains of *P. falciparum* with different degrees of drug resistance. Areas lax in antimalarial regulations tend to have higher degrees of drug resistance due to improper usage of available drugs. Areas with strict guidelines on the drugs have strains with less drug resistance (Yotoko and Elisei 2006). A small number of *falciparum* strains have the ability to form rosettes, which consist of an

infected RBC surrounded by other healthy ones. Clinically, this adaptation is very problematic, but in terms of evolution, it is quite beautiful. The rosettes are much larger than a single RBC, and thus do not fit through the microvasculature leading to the spleen, an organ that is very efficient at eliminating merozoites from RBCs. In addition to evading the spleen, the infected RBC is shielded from the host's immune system by the bubble of non-antigen-presenting RBCs. The existence of these rosettes is currently the single definitive test confirming severe childhood malaria (Chang and Stevenson 2004).

P. ovale is much less dangerous than its lethal cousin *falciparum*, and is endemic in only a small number of areas. It is closely related to *P. vivax*, and the two species are typically treated identically with little need to clinically distinguish between the two. Neither of the two is responsible for large amounts of malaria-caused mortality. However, *P. vivax* frequently relapses unless a very aggressive treatment is given upon infection. The cause for the highly probably relapses lies in its life cycle. Unlike *falciparum*, not all of the parasites leave the liver. In fact, some persistent *vivax* pathogens remain in the liver as dormant hypnozoites, and can cause relapses for years after the initial infection. Although blood tests may show no traces of *vivax*, these hypnozoites can remain in the liver undetected for up to five years and cause relapses at any time (Radloff *et al* 1996).

P. malariae is the least studied of the four *Plasmodium*, due to its status as a "benign malaria." It is even less deadly that *vivax* and *ovale*. Infection with *P. malariae* is characterized by fevers recurring in three-day intervals, making it a tertiary malaria. This three day cycle distinguishes it from *falciparum, vivax,* and *ovale*, which cause secondary malarias that occur in two-day-cycles. *P. malariae* may be the least deadly species, but it

is also the most persistent. Some patients infected with *malariae* may have the desease for the rest of their lives. Although *falciparum* is the most deadly, the other species can, on occasion, indirectly kill hosts through complications with fevers, enlarged spleens, or nervous system damage. In addition, they are remarkably persistent and can dramatically reduce a host's quality of life.

Upon an infected female *Anophales* taking a blood meal from a host, parasites enter the bloodstream and quickly invade liver cells. After this migration to the liver, there is a calm before the storm that lasts between 7 to 30 days. This incubation period tends to be shortest in *P. falciparum* and longest in *P. malariae* (CDC Malaria Factbook). The "classical" presentation of uncomplicated malaria is a 6-10 hour progression of three stages. First comes the cold stage, aptly named, due to the patient feeling cold and shivering. This progresses into the hot stage, which includes fevers, headaches, vomiting, and occasional seizures. Finally, the sweat stage occurs, in which patients sweat and eventually restore normal body temperature. These cycles have a period of two days in *P. falciparum, vivax,* and *ovale,* and periods of three days in *malariae*. Although this is the classical presentation, it is rarely observed because symptoms and stages are typically not so explicit and mutually exclusive. More frequently, an obscure combination of all three stages is observed which include fever, chills, sweats, headaches, nausea, vomiting, and body aches. Infection with *falciparum* is often characterized by an increased respiratory rate, liver enlargement, and mild jaundice. These symptoms are hardly exclusive to malaria, and a variety of maladies would present clinically with at least one of these very common symptoms. This can create complications when treating individuals living in areas not thought to be at risk of malaria. American clinicians faced with a patient

infected with malaria may immediately give a diagnosis of a common cold unless they that the patient was recently out of the country.

Severe infection occurs when a basic infection is accompanied by organ failure or other irregularities in the blood or metabolism. Cerebral malaria can occur and cause seizures, abnormal behavior, or a plethora of neurological abnormalities. Severe anemia and hemoglobinurea may be observed due to the mass destruction of RBCs. Pulmonary edema, acute respiratory distress syndrome, cardiovascular collapse, decreased blood coagulation abilities, and shock may also occur. Presentation can also include renal failure, metabolic acidosis, coagulation failure and hypoglycemia. In this model, we account for the effects of metabolic acidosis and hypoglycemia. The extent of a host's immunity to the disease plays a large role in the severity of infection and clinical findings.

Malaria is typically not difficult to diagnose in a lab. An objective microscope can be used to analyze thick or thin blood smears. Thick blood smears are more conclusive, but are also more difficult to read. Clinicians in many developing countries sometimes lack expertise in analyzing thick smears, so they often choose thin smears instead. Concluding that a patient has malaria takes different amounts of tests and time depending on the area. Hospitals in located in malaria-endemic regions will quickly give a diagnosis of malaria, while in malaria-free areas, doctors may require much more time to correctly diagnose the patient. This is simply a result of doctors knowing the likelihood of a malarial infection in that given area.

Treatment of malaria depends on the species of *Plasmodium*, location of infection, extent of drug resistance, existence of other medical problems, drugs being

taken by a patient and whether or not the patient is pregnant. The most common drugs include chloroquine and quinine but, as mentioned, are becoming less useful as *Plasmodium* evolves drug resistance to them. Some brand name drugs include Malarone, Lariam, Aralen, and Fansidar. Although not legal in the US, artemisin derivatives are also used. Most drugs specifically target the active form of the pathogen in the blood, and do little to fight other stages. Primaquine is an exception that targets hypnozoites, and is useful in eradicating persistent liver life stages and preventing relapse.

Due to the complexly intertwined nature of interactions between pathogen and host, we developed a system of differential equations to model morbidity of malaria. A previous model published by Clark *et al* was used as a foundation upon which complexities were added (2004). The process of building the model required a proper balance between creating one that was too simplified to shed light on our problem while keeping it from becoming so complex as to prevent meaningful analysis of our results. McKenzie (2000) adequately describes the process of useful modeling of malaria as follows:

> The utility of a malaria model depends not so much on how well a mathematical job has been accomplished as on how well a particular biological question has been translated, how thoroughly each assumption and its consequences have been tested, how carefully the range of relevance has been bounded, how closely descriptions and predictions fit data and the broader purpose, and how much its development has suggested explanations and deepened biological understanding.

No model can account for every possible factor of the system it describes for two reasons. First, if the model allowed any analysis whatsoever, the results would surely be trivial because one could never clearly understand the origins of results. Whether or not interesting findings were caused by a significant relationship in the model, or mere complications of the mathematics cannot be known. Second, even if one wanted to develop a model of malaria that accounts for every detail of an infection, it could not be done. At this time, knowledge of malaria has a long way to come. Many pathways, pathogen behavior, host responses, and other complexities are yet to be understood.

In order to model malaria, or any other biological system, some degree of uniformity of Nature must be assumed. Without being optimistic in regards to the uniformity of the system, a mathematical model cannot be constructed. Many of these issues were avoided when modeling by keeping our questions in mind when constructing our model. By looking at malaria through a focus on morbidity and mortality, we struck a balance between simplicity and complexity.

Clarke *et al* argue that malaria and bacterial sepsis have many features in common. Upon infection with *Plasmodium falciparum*, the most deadly malarial parasite and therefore the one we will focus on, an inflammatory response is initiated in the host. The inflammation has both beneficial and detrimental effects. On one hand, some of the inflammatory agents help defend the host from the parasite by killing *P. falciparum* inside RBCs. On the other hand, this response can be fatal, as the majority of malaria-infected patients actually die from the actions of their own immune responses, not from the parasite directly. One key player in this response is nitrous oxide (NO), which simultaneously alleviates inflammation while damaging the host's DNA. NO can also

have pathological effects on the host by damaging erythrocyte Na^+-K^+-ATPase, the bodies primary protein for maintaining electrochemical gradients inside cells. The proper functioning of this protein pump in RBCs allows the cell to maintain the correct osmolarity. When this pump fails, the intracellular charge becomes atypically hypo-osmotic. Water then moves inside the cell via osmosis, thus increasing the cell's size. When this enlarged RBC moves through the capillaries of the spleen, it is destroyed, releasing free hemoglobin into the blood stream. This process occurs on a vast scale in severe *Plasmodium* infection, and is the primary cause of anemia, hemoglobinurea, renal failure, pulmonary edema, and other typical symptoms of malaria. Dondorp et al (1999) analyzed the deformability of RBCs in patients infected with *P. falciparum*. By applying sheer stress, a force similar to the one encountered by cells moving through the spleen, they quantified the ability of the cells to deform, or squeeze through the sinusoids of the spleen. It is interesting that lack of RBC deformity in patients was well correlated with the clinical degree of anemia with which the patients presented. Parasitemia in these patients did not correlate with level of anemia. While it is not impossible that anemia and RBC deformity are merely correlated, several labeling studies suggest that they are causative. It is quantitatively obvious that the anemia observed in *P. falciparum* is not merely a result of the destruction of parasitized erythrocytes. In the same spirit as William Harvey's when he discovered the physiology of blood circulation, the numbers simply do not add up. Even if every infected RBC in the host were to suddenly burst, this event surely would not cause anemia on the scale seen in malaria. The root cause this anemia is the destruction of RBCs not by actions of a parasite, but instead by patient's bodies. This result is exacerbated by a decrease in erythropoesis. The cause of this

decline is not well understood, but it is believed that it is caused by a combination of a decrease in RBC proliferation, differentiation and maturation.

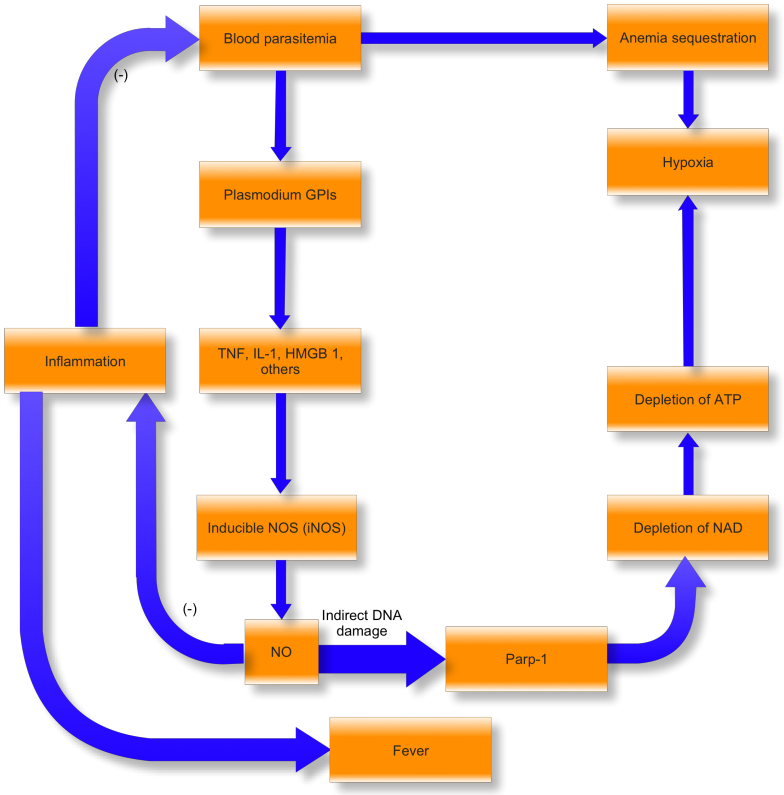

Figure 1: Basic schematic of morbidity in malaria.

As mentioned, NO can also cause small nicks in a patient's DNA. To repair this DNA damage, the host enlists the help of PARP 1, a DNA-repair enzyme that, when hyperactive, can deplete host ATP. This ATP depletion leaves the host's cells unable to perform basic homeostatic functions. Further, NO damages Na^+-K^+-ATPase function. The effects of this damage are most pronounced in RBCs, which swell as a result of disrupted osmolarity. The resulting loss of O_2 via the unnaturally high rate of healthy RBC clearance in the blood intensifies the DNA-damage-induced lack of ATP described above. See *figure 1*.

Model

Red blood cells (x) are produced via erythropoesis at rate Λ, and have several fates. The body's primary mechanism of removing RBCs is the spleen. Red blood cells change the proteins being expressed on their cell membranes as they age in order to be recognized and destroyed by the body's immune system at rate $\mu_x x$. This process eliminates old RBCs, and many of the products of phagocytising the old cells are recycled. These remains are reused as new RBCs mature. In addition, some RBCs die outside the spleen. These processes represent the normal behavior of RBCs. When infected with *Plasmodium*, however, merozoites invade RBCs. Healthy cells become infected at rate βmx. In addition, erythrocytes die en masse by the pathogenic effects of NO on their membrane Na^+-K^+-ATPase pumps, and are described in our model as a Hill function. This effect is of particular interest. Infected RBCs (y) are removed via processes similar to the ones of uninfected RBCs. They are removed at rate $\mu_y y$, and are also susceptible to NO-induced Na^+-K^+-ATPase damage. The concentration of free merozoites (m) in the blood depends on the bursting of RBCs. Each time an erythrocyte bursts, new merozoites are introduced into the blood at rate $r\mu_y y$ where they will eventually either invade a new RBC at rate βmx, or die while at rate $\mu_m m$. The concentration of TNF (f) is positively correlated with the extent of infection, and is produced at rate $ay(t-\tau)e^{-jk}$. The protein is removed via breakdown dependent on its half-life, at rate $\mu_f f$. iNOS (j) is produced as a response to TNF at rate bf, and removed at rate $\mu_j j$.

Mathematically, these interactions are modeled by the system of differential equations presented below:

$$\begin{cases} \frac{\mathrm{d}x}{\mathrm{d}t} &= \Lambda - \mu_x x - \beta m x - \frac{\alpha j^s}{\gamma^s + j^s} x, \\ \frac{\mathrm{d}y}{\mathrm{d}t} &= \beta m x - \mu_y y - \frac{\alpha j^s}{\gamma^s + j^s} y, \\ \frac{\mathrm{d}m}{\mathrm{d}t} &= r\mu_y y - \mu_m m - \beta m x, \\ \frac{\mathrm{d}f}{\mathrm{d}t} &= a y(t-\tau) e^{-jk} - \mu_f f, \\ \frac{\mathrm{d}j}{\mathrm{d}t} &= bf - \mu_j j. \end{cases} \quad (1)$$

With variables defined as follows:

Variable	Interpretation	Units
x	Concentration of healthy RBCs	Cells/μL
y	Concentration of infected RBCs	Cells/μL
m	Concentration of free merozoites	Cells/μL
f	Concentration of TNF	pM
j	Concentration of iNOS	pM

Parameters are given below:

Parameter	Interpretation	Value	Units
Λ	Rate of erythropoesis	26,560	cells/(μL*hours)
μ_x	Removal rate of RBCs via spleen	0.0083	1/hours
β	Contact (infection) rate between merozoites and healthy RBCs	$8x10^{-6}$	μL/(cells*hours)
μ_y	Removal rate of infected RBCs	0.025	1/hours
r	Number of free merozoites released per bursting RBC	24	cells
μ_m	Death rate of free merozoites	60	1/hours
α	Maximum percentage of RBCs killed via spleen due to NO induced Na^+-K^+-ATPase damage (supremum of hill function)	0.8	1/hours
γ	Threshhold for dramatic NO induced Na^+-K^+-ATPase damage (offset of hill function)	1	[iNOS] in pM
s	Speed at which $\alpha \to 100$ once Υ is reached (steepness of hill function)	2	N/A
a	Default rate of TNF upregulation	10	pM/(cells*hours)
k	TNF downregulation due to feedback of NO	0.1	1/pM
μ_f	Rate of TNF degradation	3.47	1/hours
μ_j	Rate of iNos degradation	0.347	1/hours
b	iNOS upregulation rate due to TNF	1	1/hours
τ	Delay of TNF effect onset	2	hours

Model analysis

Theorem 1: For all t, x(t), y(t), m(t), f(t), j(t) ≥ 0

Proof Let $h(j) = (\alpha j(t_i)^s)/(\gamma^s + j(t_1)^s)$

where *i* is the Case number.

The proof consists of five cases, one for each variable, and in the *i*th case we assume that the there exists a time t_i that is the first time at which the variable attains the value zero and has negative derivative. We then prove by contradiction that no such t_i can exist and therefore all of the variables stay nonnegative for all t.

Case 1: Assume $x(t_1) = 0$ and $x'(t_1) < 0$

Then

$$x'(t_1) = \Lambda - \mu_x x(t_1) - \beta x(t_1) m(t_1) - h(j) x(t_1) < 0$$
$$\implies \Lambda - x(t_1)[\mu_x + \beta m(t_1) + h(j)] < 0$$

which is a contradiction because $x(t_1)=0$ and $\Lambda>0$ by definition. Thus for all t, $x(t)\geq 0$.

Case 2: Assume $y(t_2) = 0$ and $y'(t_2) < 0$

Then

$$y'(t_2) = \beta x(t_2) m(t_2) - \mu_y y(t_2) - h(j) y(t_2) < 0$$
$$\implies \beta x(t_2) m(t_2) - y(t_2)[\mu_y + h(j)] < 0$$

which can only be true if $m(t_2) < 0$ since $x(t_2)$ is nonnegative by Case 1. This brings us to Case 3.

Case 3: Assume $m(t_3) = 0$ and $m'(t_3) < 0$

Then

$$m'(t_3) = r\mu_y y(t_3) - \mu_m m(t_3) - \beta x(t_3) m(t_3) < 0$$
$$\implies r\mu_y y(t_3) - m(t_3)[\mu_m + \beta x(t_3)] < 0$$

which can only be true if $y(t_3) < 0$. Thus in Case 2, $m(t_2) < 0$ and in Case 3, $m(t_3) = 0$, so $t_3 < t_2$. However, in Case 3, $y(t_3) < 0$ and in Case 2, $y(t_2) = 0$, so $t_2 < t_3$, which is a contradiction. Thus for all t, $y(t) \geq 0$ and $m(t) \geq 0$.

Case 4: Assume $f(t_4) = 0$ and $f'(t_4) < 0$

Then

$$f'(t_4) = a y(t_4 - \tau) e^{-jk} - \mu_f f(t_4) < 0$$

which is a contradiction because $f(t_4) = 0$ and $y(t_4 - \tau) > 0$ by Case 2.

Case 5: Assume $j(t_5) = 0$ and $j'(t_5) < 0$

Then

$$j'(t_5) = b f(t_5) - \mu_j j(t_5) < 0$$

which is a contradiction because $j(t_5) = 0$ and $f(t_5) > 0$ by Case 4. Thus, all variables are non-negative.

Theorem 2: All variables (x(t), y(t), m(t), f(t), j(t)) are bounded.

that is, $\limsup_{t\to\infty} x(t) \leq \Lambda/\mu_x$, $\limsup_{t\to\infty} y(t) \leq \Lambda/\mu_*$ *where* $\mu_* = min(\mu_x, \mu_y)$, $\limsup_{t\to\infty} m(t) \leq r\mu_y y/\mu_m$, $\limsup_{t\to\infty} f(t) \leq ay(t-\tau)e^{-jk}/\mu_f$. *and* $\limsup_{t\to\infty} j(t) \leq bf/\mu_j$.

Proof We already know that all parameters and variables are nonnegative by the definition of our parameters and the nonnegativity proof for our variables.

To prove that $x(t) \leq \Lambda/\mu_x$, suppose otherwise. Suppose there exists a time t_x at which $x(t_x) > \Lambda/\mu_x$. Then, by the continuity of our functions, there has to exists a time $t_p < t_x$ such that $x(t_p) = \Lambda/mu_x$. We know then that $[x(t_x) - x(t_p)]/[t_x - t_p] > 0$, which implies that there exists a time t_q such that $t_p < t_q < t_x$, $x'(t_q) > 0$, and $x(t_q) > \Lambda/\mu_x$. However, this is a contradiction because we also have that $x'(t_q) < 0$ by the fact that for all $x(t) > \Lambda/\mu_x$, $x'(t) \leq \Lambda - \mu_x x < 0$. Thus $\limsup_{t\to\infty} x(t) \leq \Lambda/\mu_x$.

To prove that $y(t)$ is bounded, consider $(x+y)'(t)$. We know that $(x+y)'(t) \leq \Lambda - \mu_*(x+y)$ where $\mu_* = min(\mu_x, \mu_y)$. Thus, using an argument similar to the one that proved boundedness for $x(t)$, $\limsup_{t\to\infty}(x+y)(t) \leq \Lambda/\mu_*$. Thus also $\limsup_{t\to\infty} y(t) \leq \Lambda/\mu_*$. Since we've already proven $x(t)$ is bounded, $y(t)$ must also be bounded.

To prove that $m(t)$ is bounded, note that $m'(t) \leq r\mu_y y - \mu_m m$. Thus, using an argument similar to the one that proved boundedness for $x(t)$, $\limsup_{t\to\infty} m(t) \leq r\mu_y y/\mu_m$. Since we've already proven $y(t)$ is bounded, $m(t)$ must also be bounded.

To prove that $f(t)$ is bounded, note that $f'(t) = ay(t-\tau)e^{-jk} - \mu_f f$. Thus, using an argument similar to the one that proved boundedness for $x(t)$, $\limsup_{t\to\infty} f(t) \leq ay(t-\tau)e^{-jk}/\mu_f$. Since we've already proven $y(t)$ is bounded, $f(t)$ must also bounded.

To prove that $j(t)$ is bounded, note that $j'(t) = bf - \mu_j j$. Thus, using an argument similar to the one that proved boundedness for $x(t)$, $\limsup_{t\to\infty} j(t) \leq bf/\mu_j$. Since we've already proven $f(t)$ is bounded, $j(t)$ must also be bounded.

Equillibria for the model can be found by setting the partial differential equations equal to zero. In addition, the Hill function may be simplified to allow for simpler analysis. This yields the following set of equations:

$$\begin{cases} x' &= \Lambda - \mu_x x - \beta m x - \alpha j x, \\ y' &= \beta m x - \mu_y y - \alpha j y, \\ m' &= q r \mu_y y - \mu_m m - \beta m x, \\ f' &= a y(t-\tau) e^{-kj} - \mu_f f, \\ j' &= bf - \mu_j j. \end{cases} \tag{2}$$

The In order to linearize the system, we take the Jacobian matrix of the simplified model above. This yields

$$J = \begin{pmatrix} -(\mu_x + \beta m + \alpha j) & 0 & -\beta x & 0 & -\alpha x \\ \beta m & -(\mu_y + \alpha j) & \beta x & 0 & -\alpha y \\ -\beta m & r\mu_y & -(\mu_m + \beta x) & 0 & 0 \\ 0 & a e^{-kj} & 0 & -\mu_f & -aky e^{-kj} \\ 0 & 0 & 0 & b & -\mu_j \end{pmatrix}$$

Upon obtaining this result, the following may be stated:

Theorem 1: let us define

$$R_0 = \frac{\beta \Lambda (r-1)}{\mu_m \mu_x}$$

Then for $R_0 < 1$, the disease free equilibrium defined as $(\Lambda/\mu_x, 0, 0, 0, 0)$ is locally asymptotically stable.

Proof: The Jacobian matrix simplifies to

$$J = \begin{pmatrix} -\mu_x & 0 & -\frac{\beta\Lambda}{\mu_x} & 0 & -\frac{\alpha\Lambda}{\mu_x} \\ 0 & -\mu_y & \frac{\beta\Lambda}{\mu_x} & 0 & 0 \\ 0 & r\mu_y & -(\mu_m + \frac{\beta\Lambda}{\mu_x}) & 0 & 0 \\ 0 & a & 0 & -\mu_f & 0 \\ 0 & 0 & 0 & b & -\mu_j \end{pmatrix}$$

at the disease free equilibrium. It is immediately obvious that three eigenvalues ($\lambda_3 = -\mu_x$, $\lambda_4 = -\mu_j$, $\lambda_5 = -\mu_f$) are negative. Upon finding these three eigenvalues, the Jacobian matrix may be simplified be removing the rows and columns corresponding to λ_3, λ_4, and λ_5. This yields the following sub-matrix:

$$J_1 = \begin{pmatrix} -\mu_y & \frac{\beta\Lambda}{\mu_x} \\ r\mu_y & -\mu_m - \frac{\beta\Lambda}{\mu_x} \end{pmatrix}$$

The trace of this matrix is strictly positive (because all parameters are non-negative). Calculating this determinant yields

$$\mu_y(\mu_m + \frac{\beta\Lambda}{\mu_x}) - \frac{r\mu_y\beta\Lambda}{\mu_x}.$$

In order for the determinant to be greater than zero,

$$\mu_y(\mu_m + \frac{\beta\Lambda}{\mu_x}) > \frac{r\mu_y\beta\Lambda}{\mu_x}$$

Multiplying the left-hand side by r and distributing the μ_y gives

$$r\mu_\psi\mu_\mu + \frac{\rho\mu_\psi\beta\Lambda}{\mu_\xi} > \frac{\rho\mu_\psi\beta\Lambda}{\mu_\xi}$$

Which is simply

$$r\mu_{\psi}\mu_{\mu} > 0$$

The remaining criterion for the system to be locally asymptotically stable is that for $J_1 >$ 0,

$$\Leftrightarrow \mu_m + \frac{\beta\Lambda}{\mu_x} - r\frac{\beta\Lambda}{\mu_x} > 0 \Leftrightarrow 1 > \frac{\beta\Lambda(r-1)}{\mu_m\mu_x}$$

which is merely a simplification of the above inequality. W

The three eigenvalues obtained above are trivial, because they are not biologically meaningful. In order to determine the non-trivial eigenvalues, and thus the fixed points for disease free equilibrium, we subtract Iλ from the Jacobian sub-matrix, J_1. This yields the following matrix

$$J_1' = \begin{bmatrix} -\mu_{\psi} - \lambda & \frac{\beta\Lambda}{\mu_{\xi}} \\ \rho\mu_{\psi} & -\mu_{\mu} - \frac{\beta\Lambda}{\mu_{\xi}} - \lambda \end{bmatrix}$$

with its determinant being

$$\lambda^2 + (\frac{\beta\Lambda}{\mu_x} + \mu_m + \mu_y)\lambda + \mu_y(\mu_m + \frac{\beta\Lambda}{\mu_x}) - \frac{\beta\Lambda r\mu_y}{\mu_x}.$$

Define A and B such that

$$A = \frac{\beta\Lambda}{\mu_{\xi}} + \mu_{\mu} \quad \text{and} \quad B = \frac{\beta\Lambda\rho\mu_{\psi}}{\mu_{\xi}}.$$

The determinant of the matrix now becomes

$$\lambda^2 + (A + \mu_y)\lambda + \mu_y A - B$$

and solutions of lambda may be found via the quadratic equation.

$$\lambda_{1,2} = \frac{-(A + \mu_y) \pm \sqrt{(A + \mu_y)^2 - 4(\mu_y A - B)}}{2}.$$

Because biologically, $\lambda_1, \lambda_2 \in \circ$,

$$\sqrt{(A + \mu_\psi)^2 - 4(\mu_\psi A - B)} \in \circ \Rightarrow (A + \mu_\psi)^2 - 4(\mu_\psi A - B) > 0$$

implies the following conjecture:

Conjecture 1a: One $\lambda > 0$.

Conjecture 1b: The other $\lambda > 0$ *iff* $R_0 < 1$.

Model Simulations

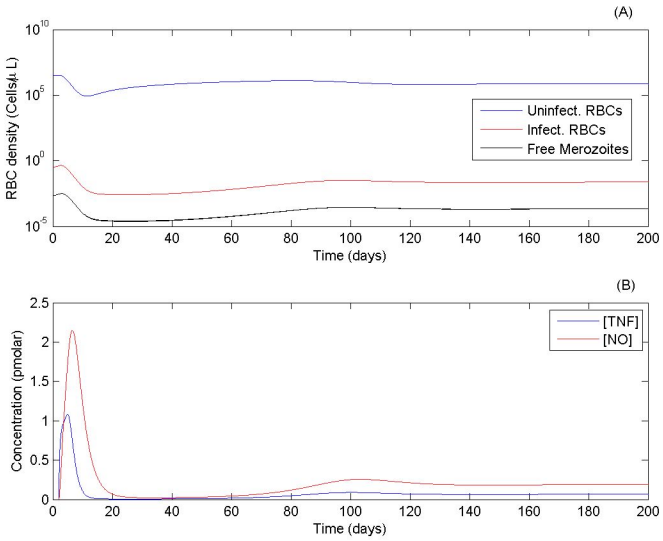

Figure 2) chronic malaria infection as predicted by our model. (a) The dynamics of RBCs, infected RBCs, and free merozoites. (b) Dynamics of TNF and NO.

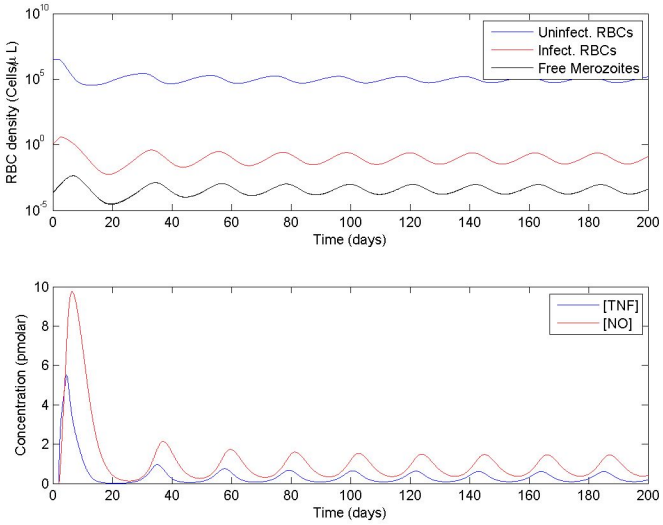

Figure 3) Sustained oscillations obtained from the model. All parameters are at their default values, except for beta = 8 x 10^{-4}.

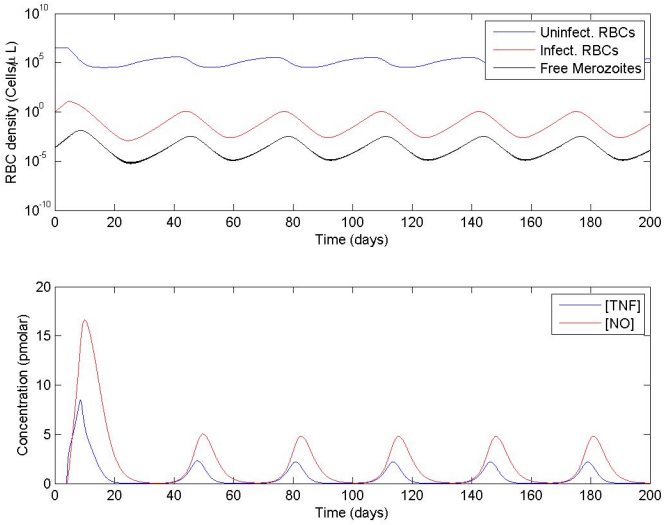

Figure 4) Changing the time delay to 4 while using the same parameters in figure 3.

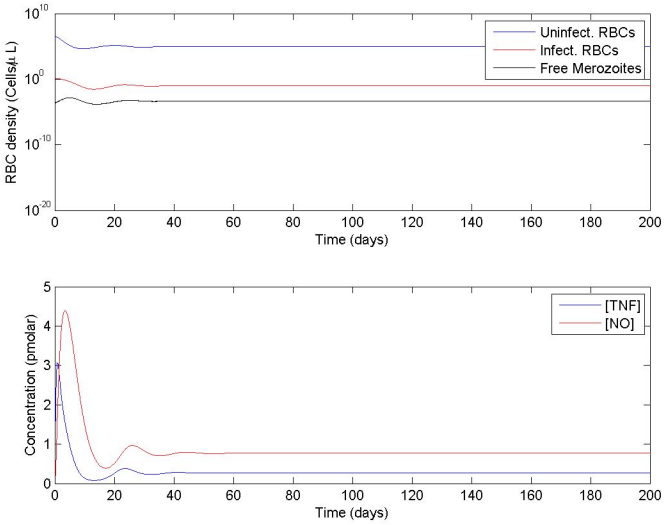

Figure 5) Removal of time delay ($\tau = 0$) severely dampens oscillations.

Of the many attributes that distinguish the four malarial parasites from one another, an important one is parasitemia. One such characteristic is the potential parasitemia each *Plasmodium* species can cause. *P. falciparum* can live in much higher densities in its hosts, and this facet is one of many competing hypotheses that attempts to

explain the differences in the clinical manifestations of different malarial parasites. Below are figures with all parameters and initial conditions at default values except for *m(0)*, at different values.

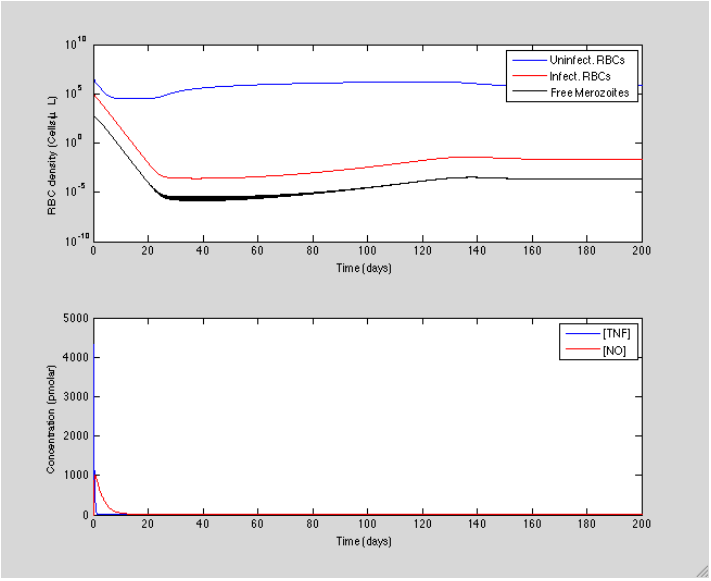

Figure 6) *m(0)*=1x10^5. Large concentrations of TNF and NO can be observed in the very beginning of the realization in the bottom panel.

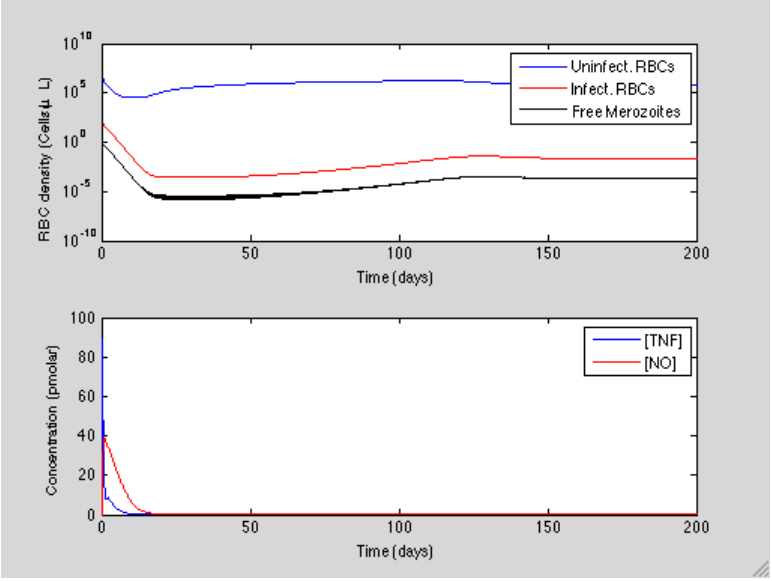

Figure 7) *m(0)*=1x10^2. Concentrations of NO and TNF are much lower than in figure 8.

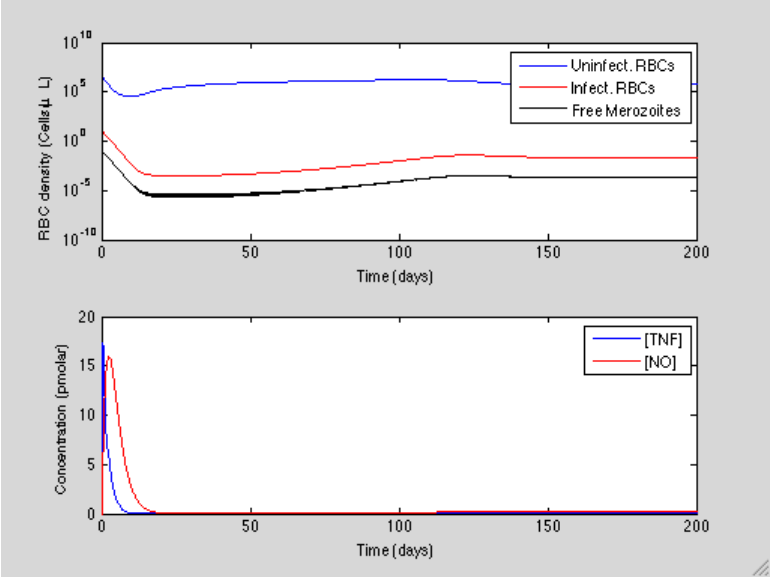

Figure 8) *m(0)*=10. Again, a smaller starting value for *m* corresponds with a decrease in [TNF] and [NO].

Next, we may look at a similar comparison of values for *m(0)*, except that beta=$1x10^{-4}$.

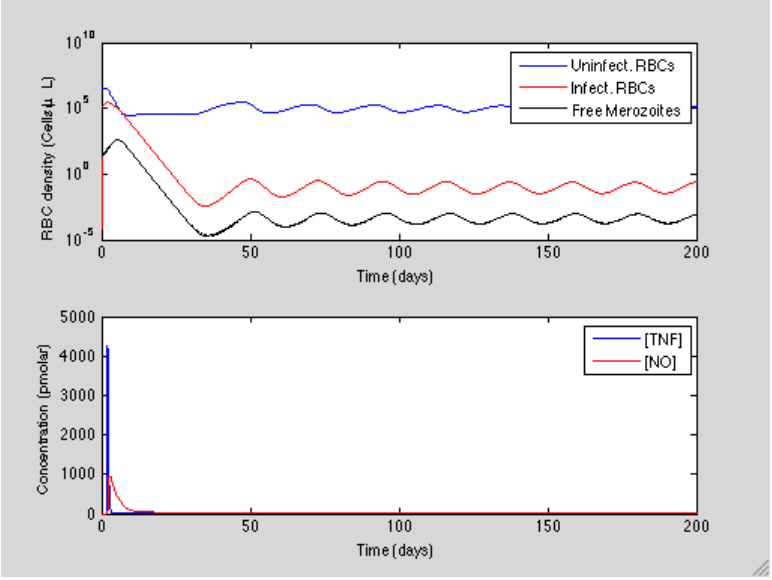

Figure 9) m(0)=$1x10^{5}$. A point exists in the top panel in which the number of uninfected RBCs equals the number of infected RBCs. This would be an extreme parasitemia.

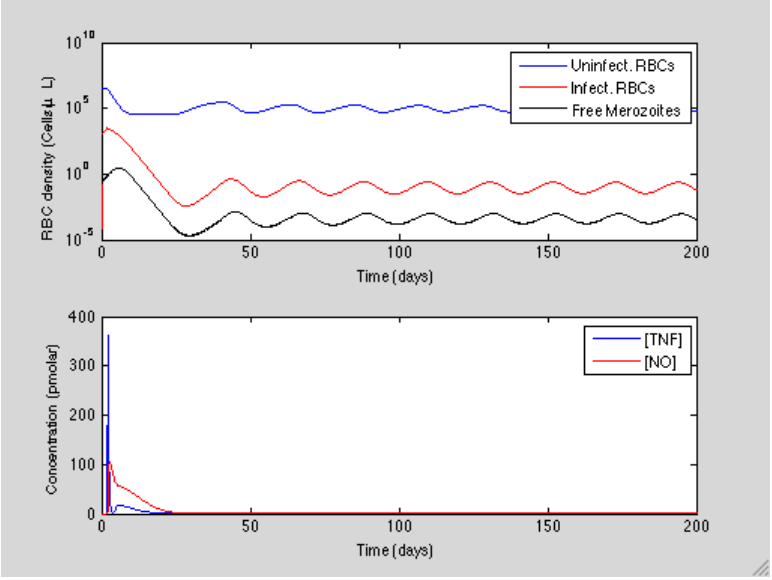

Figure 10) *m(0)*=1x10^4. Decreasing *m(0)* reduces the amplitude of the initial spikes in [TNF] and [NO].

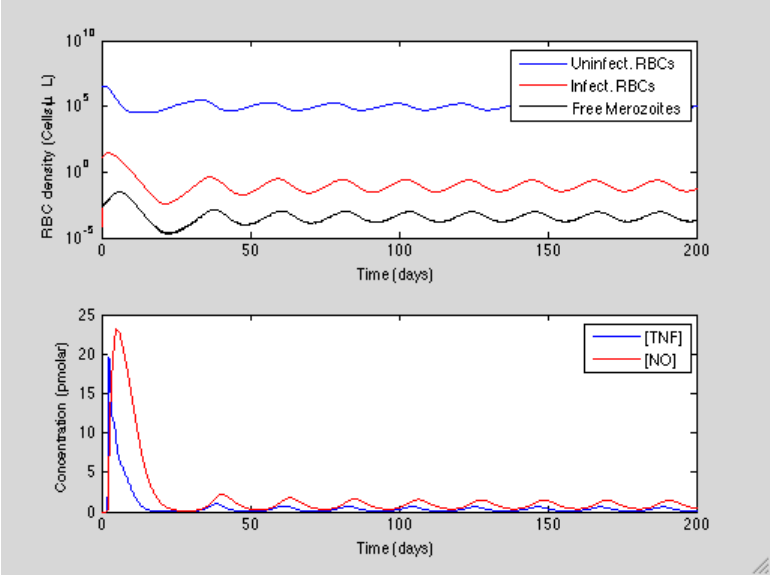

Figure 11) *m(0)*=10.

Because TNF is the first component of the NO cascade, it seems logical to explore what effects varying initial concentrations of TNF have on the host/parasite cell counts and cytokine/NO concentrations.

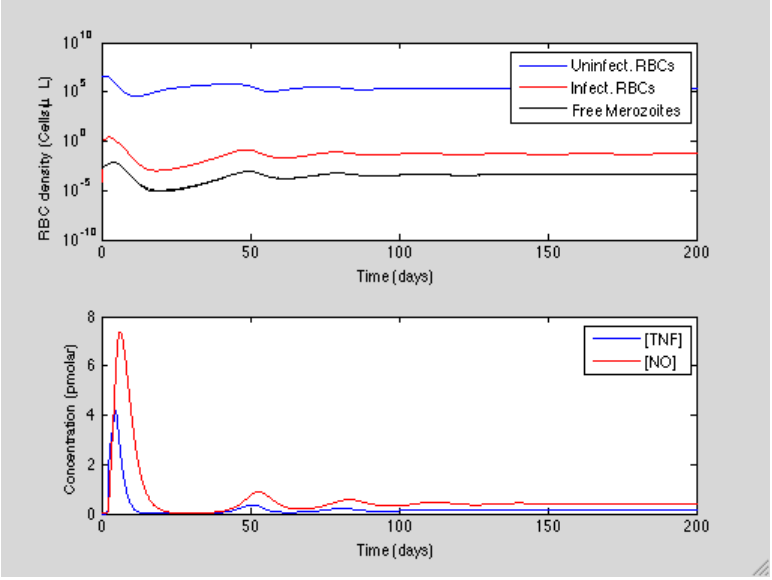

Figure 14) *f(0)*=0.01.

In the same spirit of changing values of beta presented above, below are various permutations of values for r and μ_m. These characteristics are likely to vary between species, and possibly within strains of each species. The values for r = (24, 28, 32) are permutated with values for m = (40, 60, 80). In the figures, values for r and μ_m are indicated as (r, μ_m).

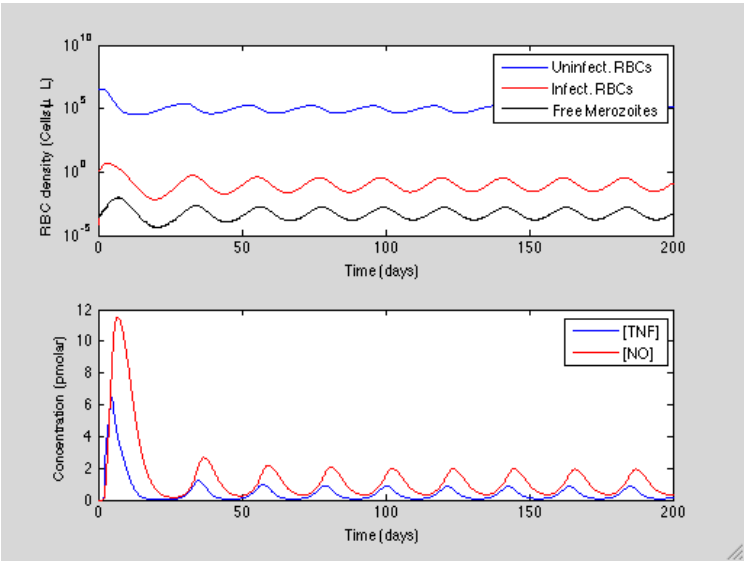

Figure 12) (28,60)

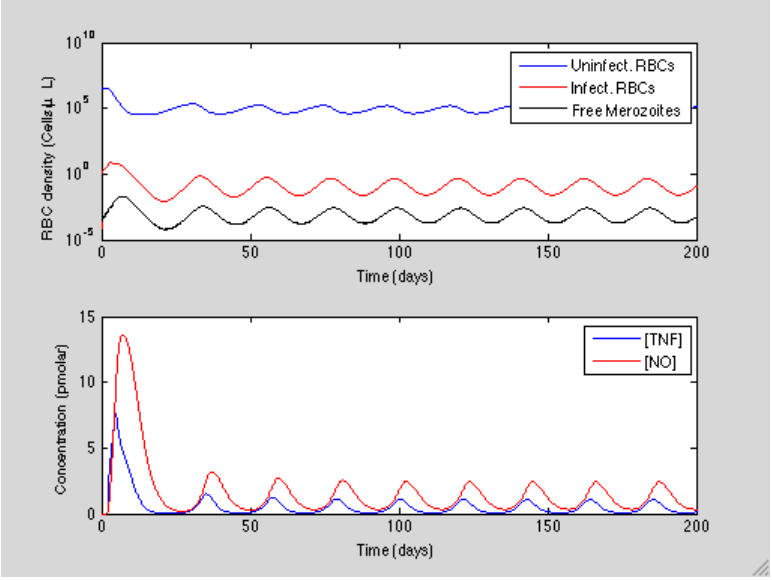

Figure 13) (32,60)

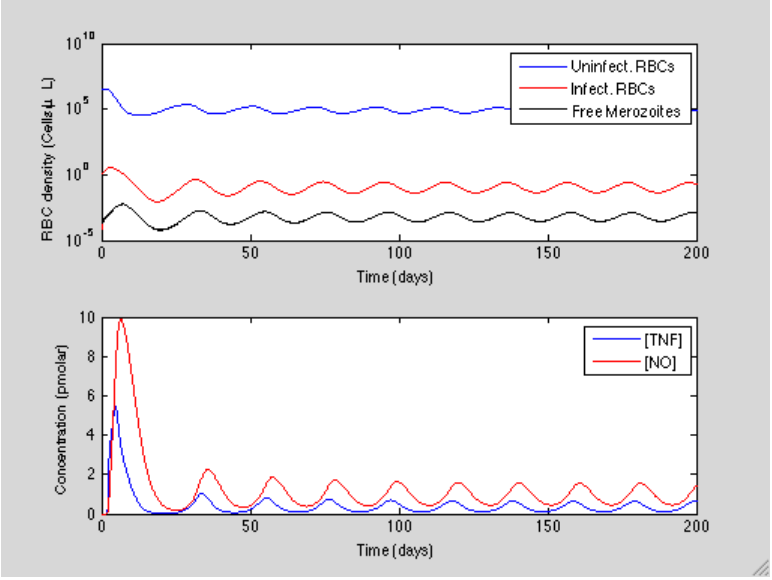

Figure 14) (24,40)

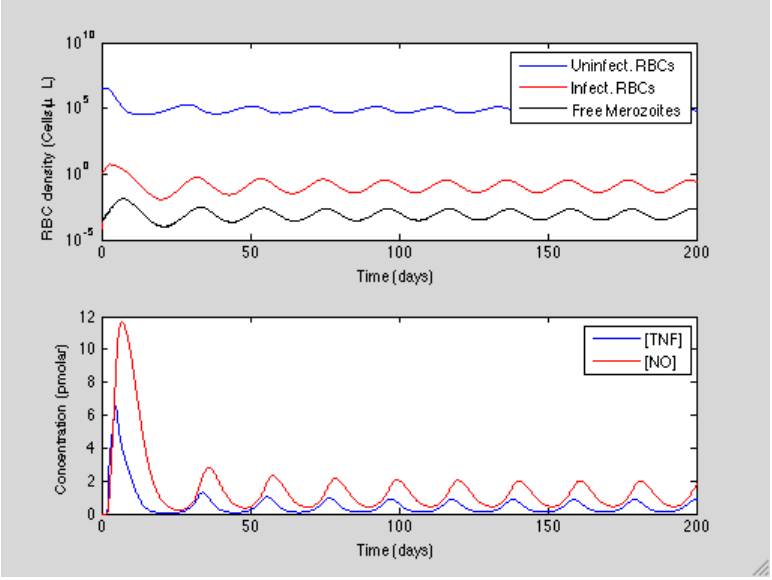

Figure 15) (28,40)

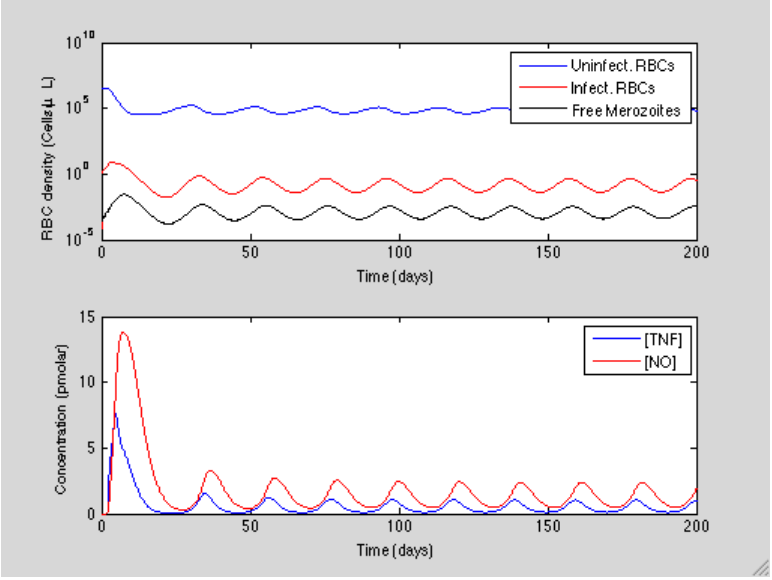

Figure 16) (32,40)

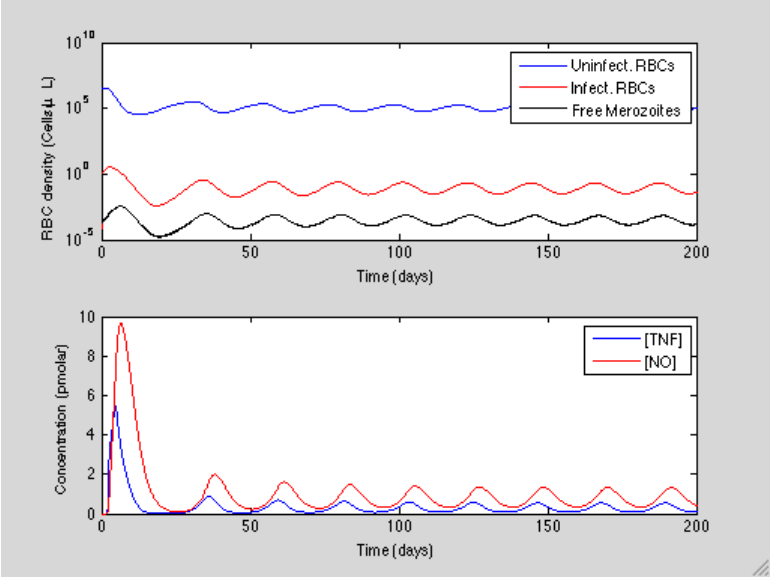

Figure 17) (24,80)

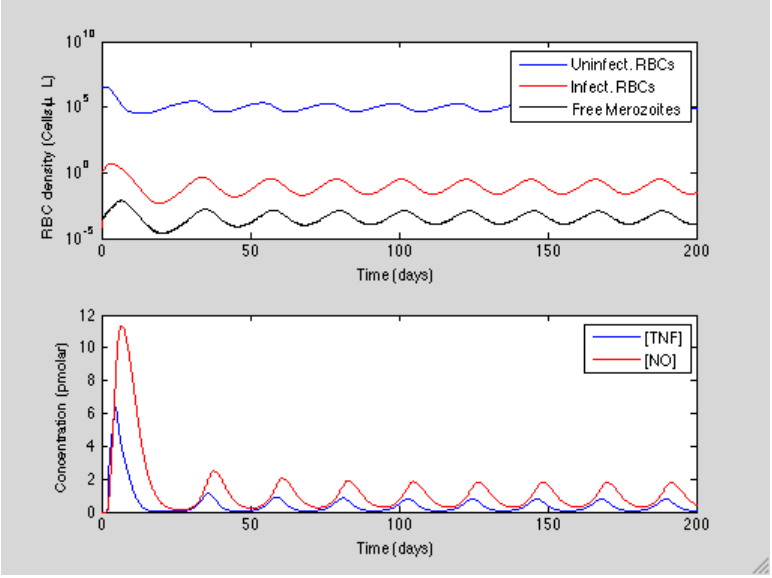

Figure 18) (28,80)

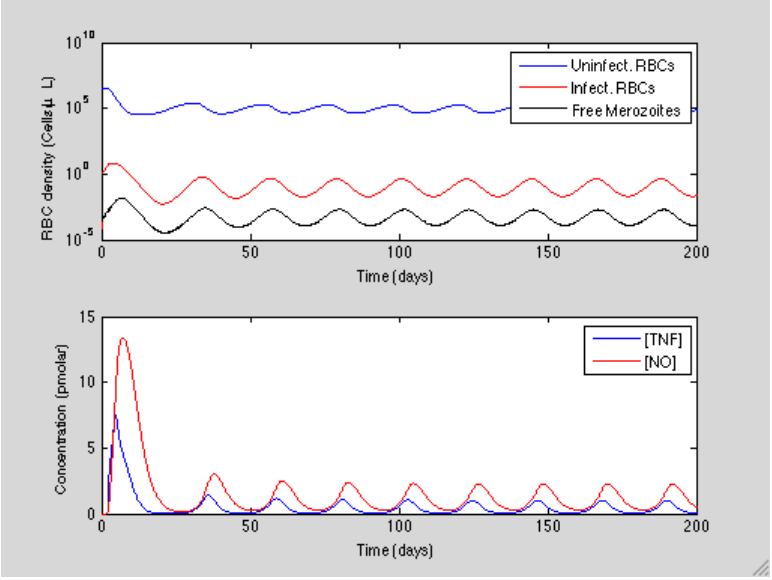

Figure 19) (32,80)

Discussion

Clark *et al* provided a reasonable framework for the more comprehensive model in this paper. Tumwiine's (2008) model is very similar to the one presented here, and not surprisingly, realizations of the two are comparable. Both models produce sustained oscillations with decreasing amplitude. This result is known to happen in typical clinical courses of malaria.

Taking a closer look at the equation for R_0, an interesting observation can be made. The presence of Λ suggests that the clinical outcome of a malaria infection can depend on the host's rate of erythropoesis. Because *Plasmodium* species rely on RBCs to live inside, it is logical that implicit spatial interactions between merozoites and host cells can affect the dynamics of the model. In simulations not shown here, increasing Λ dampens the oscillations in the system. However, the value for Λ that effectively removes the oscillations is outside the bounds of biological relevance because such a rate of

erythropoesis is greater than the average value for Λ by orders of magnitude. μ_x plays a similar role being in the denominator or R_0. Almost surely, there is an optimal ratio of RBC production to clearance such that the decrease in host functionality is minimal while limiting a *Plasmodium* infection. More work will need to be done in order to prove this conjecture. Increasing Λ does not change the behavior of the cytokines or NO. Why changing Λ affects the dynamics of the cells in the model while not producing visible changes in cytokines or NO dynamics is unknown.

The first eigenvalue found for the disease free equilibrium is always positive. That is, there is always at least one fixed point in the model. The second eigenvalue is only positive (and therefore relevant) if $R_0 > 0$.

Figure 2 shows a simulation of the model when all parameters are at their default value. This graph is not biologically interesting on its own, but when compared to the other figures, the differences are noteworthy. It is immediately obvious that this system does not oscillate; the curves are quite flat. Also note how similar the curves for the number of uninfected RBCs, infected RBCs and merozoites are. The primary difference is that they appear to be vertical transformations of each other. One would expect that the number of uninfected RBCs would decrease as the number of infected cells increased, but that is not the case here. The curves for TNF and NO are similar. NO's resembles TNF's multiplied by some scalar. This result is reasonable in the model, since NO is produced as a direct response to circulating TNF. Conversely, NO's curve should decrease as TNF's does. This is clearly the case.

By merely changing β to $1x10^{-4}$, a dramatic increase can be seen (figure 3). Oscillations are introduced that gradually decrease in amplitude with time. That is,

$\limsup_{t\to\infty}(\mu(\tau))$ and $\limsup_{t\to\infty}(\psi(\tau))$ are strictly decreasing while $\liminf_{t\to\infty}(\mu(\tau))$ and $\liminf_{t\to\infty}(\psi(\tau))$ are strictly increasing.

This pattern can be interpreted biologically as the immune system slowly defeating the *Plasmodium* parasite. Each peak in merozoites and infected RBCs is taller than the next. The curves do not resemble mere transformations of each other in two respects. First, the number of uninfected RBCs is negatively correlated with the number of infected RBCs and free merozoites. This is an elegant result because it simply makes sense in terms of biology. Removing RBCs from the healthy pool by infecting them should show this inverse correlation. The second difference is that the peaks of the uninfected RBC curve do not perfectly match up with the troughs of the infected RBC and merozoites curves. The single-cycle maxima and minima of uninfected RBCs correlates with the intermediate values of infected RBCs and merozoites. This offset is approximately two hours. While τ may be set at 2 hours, this result is not trivial because it was increasing β that caused oscillations. Also, the initial spikes in [TNF] and [NO] are much taller in amplitude by increasing β.

In figure 4, doubling the delay τ to 4 hours increases [TNF] and [NO] drastically. Oscillations are visible within the troughs of the free merozoites curves. It is difficult to say whether this is an artifact of the model or a legitimate biological occurrence.

Figure 5 concludes the elementary analysis of the model and shows the results of a simulation when the time delay is eliminated from the model. Oscillations appear only in the beginning of the realizations, and are essentially removed after two cycles. Cell counts in figure 5a change very little while the concentrations in figure 5b decrease markedly.

Simulations were run in order to see the effects of various initial conditions for *m* while leaving β at its default value. The purpose of leaving β at a small value was to see how changing initial parasite loads affected the dynamics of the model. No oscillations were introduced, nor were they expected. As in the other figures, cell counts remain semi-constant despite changing *m*'s order of magnitude. The concentrations of TNF and NO were dramatically affected, however, and some values are probably outside the range of biological significance. This is especially true in the first figure, which shows concentrations in the thousands of picomolars. The shapes of the curves change very little throughout the different values for $m(0)$ except for the initial dynamics in of [TNF] and [NO].

A similar analysis was performed, but with a larger value for β. The results obtained are much more interesting than those that use a default value for beta. In a realization corresponding to a severe *falciparum* malaria infection, or the maximum possible parasitemia of *vivax,* or *ovale, t*he dynamics in are especially significant. The number of infected RBCs rapidly increases in the very beginning of the graph. The number of free merozoites rises for a short time after this, until it reaches its supremum limit shortly after $t = 0$. Near this point in time, all three cell counts decrease and quickly each their infimum limits. There are no oscillations during this period of time, and they only begin once all three functions have hit their infimum limits. The most interesting result of this figure is that there is a point at which $y(t) = m(t)$. It is also interesting that regardless of the value for $m(0)$, there was no point at which $y(t) < m(t)$ (realizations not shown here). Simulations with decreased $m(0)$ exhibit similar behavior, with the only difference in cell dynamics being that $y(t)$ and $m(t)$ are shifted down in the graph. The

dynamics of [TNF] and [NO] are also different. There is still a sharp spike in [TNF] at the beginning, but unlike the other figures, there is a much smaller spike immediately after this one. There may be oscillations in the very first portion of the graph, but they are rapidly dampened. The point of the second spike in [TNF] corresponds with an increase in the slope of [NO]. Note that the spike in *f(t)* does not cause *j'(t)* to become positive, but instead, less negative. The concentrations of both species quickly stop oscillating after this.

Changing the value for *f(0)* yields surprisingly similar results. The graph corresponding to the largest initial concentration in TNF is the only one with obvious differences from the others. The first unexpected observation is that [TNF] and [NO] are actually lower in this graph. While [TNF] starts at a larger initial value, it quickly decreases. This may correspond to a high concentration of TNF limiting the initial growth of merozoites which then do not provoke such an intense immune response, thus decreasing concentrations of TNF and NO. Whether or not high baseline concentrations of TNF in patients actually corresponds with a decrease once infected with *Plasmodium* is empirically unknown. However, this is one key finding that could have clinical implications. Increasing r while holding μ_m at 60 has little effect on cell dynamics, but it increased the concentrations of both NO and TNF. This is noteworthy because it may represent the host's body limiting the dynamics of the infection and merozoites via increasing the concentrations of NO and TNF. These increases in concentration had the effect of keeping *x(t), y(t),* and *m(t)* stable regardless of the value for r. Repeating the same procedure while holding *m(0)* at 40 and 80 yielded the same result. The host's immune system reacted in such a way that it offset the increases in r, and kept the cell

dynamics the same. Holding r constant at 24 while increasing μ_m has little effect on the dynamics of the system.

Varying the value for μ_x had a remarkably small effect. Running these simulations was done in order to see if different values for μ_x could have an effect on the dynamics via the effects of implicit space in the model. Changing the parameter did not facilitate any limiting behavior on the merozoites due to interactions/competition for RBCs.

In conclusion, it is obvious that the oscillations of the system are introduced by the time delay. Beta played a significant effect on the behavior of the oscillations. By increasing the contact-infection rate between RBCs and free merozoites, the amplitude of the oscillations is increased. This result is to be expected both mathematically and biologically. Regardless of how large beta is, no oscillations are seen without the time delay. An increased initial condition for *f(t)* actually produced decreased concentrations of TNF and NO past the origin. Because patients infected with *Plasmodium* typically die at the hand of their own immune responses, this result could be clinically significant. It was interesting that regardless of the value for r, the host's immune system seems to have compensated for the change by altering [TNF] and [NO] to yield similar graphs of *x(t), y(t),* and *m(t)*. Changing the death rate of erythrocytes did not change any of the model's dynamics, suggesting that there is no competition between merozoites for RBCs. Many of these results are interesting with respect to both mathematics and biology, but which field of study they may be attributed to will require further research.

1. Azevedo, M.F., Portillo, H.A. (2007) *Bioinformatics in Tropical Disease Research: A Practical and Case-Study Approach.* **B01** Control of Gene Expression in *Plasmodium*.

Austerman, R.J.

2. CDC Malaria Factbook: Disease. http://www.cdc.gov/malaria/disease.htm. Accessed 4-26-2009.
3. Chang, K.H., Stevenson, M.M. (2004) Malarial anaemia: mechanisms and implications of insufficient erythropoiesis during blood-stage malaria. *International Journal for Parasitology* **34**:1501-1516.
4. Clark, I.A. *et al.* (2004) Pathogenesis of malaria and similar conditions. *Clinical Microbiology Reviews* **17**: 509-539.
5. Escalante, A.A., Barrio, E., Ayala, F.J. (1995) Evolutionary origin of human and primate malarias: evidence from the circumsporozoite protein gene. *Mol Bio Evol* **12**:616-26.
6. Goodman, C. (2007) Drug shop regulation and malaria treatment in Tanzania—why do shops break the rules, and does it matter? *Health and Policy Planning* **22**:393-403.
7. Hartl, D.L. (2004) The origin of malaria: mixed messages from genetic diversity. *Nat Rev Microbiol* **2**:15-22.
8. Joy, D.A. *et al*. (2003) Early Origin and Recent Expansion of Plasmodium falciparum. *Science* **300**:318 – 32.
9. McKenzie F.E. (2000). Why Model Malaria? *Parasitology Today* **16**:511-516.
10. Radloff, P.D. *et al*. (1996) Atovaquone plus proguanil is an effective treatment for Plasmodium ovale and P. malariae malaria. *Trans R Soc Trop Med Hyg* **90**:682.
11. Tumwiine J. *et al*. (2008) On global stability of the intra-host dynamics of malaria and the immune system. *Journal of Mathematical Analysis and Applications* **341**: 855-869.
12. Yotoko, K.S.C., Elisei, C. (2006) Malaria parasites (Apicomplexa, Haematozoea) and their relationships with their hosts: is there an evolutionary cost for the specialization? *Journal of Zoological Systematics and Evolutionary Research* **44**: 265-273.